Available online at www.sciencedirect.com
SCIENCE DIRECT®
Journal of Solid State Chemistry 174 (2003) 418–423
JOURNAL OF SOLID STATE CHEMISTRY
http://elsevier.com/locate/jssc

Transmission electron microscopy study of Ruddlesden–Popper $Ca_{n+1}Mn_nO_{3n+1}$ $n=2$ and 3 compounds

Leonid A. Bendersky,[a,*] Martha Greenblatt,[b] and Rongji Chen[b]

[a] *Metallurgy Division, NIST, 100 Burea Dr., Stop 8554, Bldg. 223/A117, Gaithersburg, MD 20899-8554, USA*
[b] *Department of Chemistry, Rutgers, The State University of New Jersey, Piscataway, NJ 08854, USA*

Received 13 September 2002; received in revised form 17 December 2002; accepted 10 May 2003

Abstract

Two Ruddlesden–Popper compounds $Ca_{n+1}Mn_nO_{3n+1}$ with $n=2$ and 3 synthesized by a citrate gel technique have been studied by TEM. The structure of $Ca_4Mn_3O_{10}$ is consistent with the previously determined structure having the space group *Pbca* and $a^-a^-c^+/a^-a^-c^+$ tilt system. The presence of defects suggests the possible high-temperature phase transition from untilted $I4/mmm$ to *Pbca*. The structure of $Ca_3Mn_2O_7$ was found to be different from the previously suggested $I4/mmm$ symmetry. $Ca_3Mn_2O_7$ forms with an orthorhombic structure with either *Cmcm* or $Cmc2_1$ space group. A structural model for $Cmc2_1$ based on the tilting of almost-rigid octahedra with $a^+c^-c^-/a^+c^-c^-$ tilt system is proposed. The lamellar defects were shown to be twin variants of the $Cmc2_1$ structure with the $(001)_t$ interfaces, which suggests the possible tilting phase transition from the ideal $I4/mmm$ to $Cmc2_1$ following the maximal group–subgroup symmetry tree: $I4/mmm \rightarrow Fmmm \rightarrow Bbmm(Cmcm) \rightarrow Bb2_1m(Cmc2_1)$.
© 2003 Elsevier Inc. All rights reserved.

Keywords: $Ca_3Mn_2O_7$; $Ca_4Mn_3O_{10}$; Manganates; TEM; Crystallography; Phase transition

1. Introduction

The Ruddlesden–Popper (RP) phases, $Ca_{n+1}Mn_nO_{3n+1}$ ($n=1,2,3$) and $CaMnO_3$ ($n=\infty$) are members of perovskite-type manganates. Many of these systems have been the subject of intense research, primarily because of their complex magnetic and electric transport properties and colossal magnetoresistance (CMR) phenomenon [1]. The idealized RP structure, $AO(ABO_3)_n$ is comprised of n-octahedra thick perovskite-like blocks $(ABO_3)_n$ separated by a (AO) layer of the rock salt structure. Thus, the $n=1,2,3\ldots$ phases are low-dimensional layer structures, while the $n=\infty$ compounds are the prototypical three-dimensional (3D) perovskites. Crystal structures of calcium manganates have been studied by different diffraction techniques, including powder X-ray and neutron diffraction [2,4–6]. Results of these structural studies are summarized in Table 1.

Poeppelmeier et al. [2] determined the structure of $CaMnO_3$ as orthorhombic perovskite with distorted MnO_6 octahedra. The *Pnma* space group and the distortions correspond to a network of tilted octahedra, with a tilt system $a^-a^-c^+$ according to the Glazer notations [3]. For the layered $(AO)(ABO_3)_n$ structures, where the octahedra in the perovskite blocks are undistorted, the symmetry is $I4/mmm$ and the lattice parameters are approximated by a $\approx a_p$ and $c \approx 2(na_p + c_{rs}) \approx 2(na_p + 1/2a_p)$, where a_p is the lattice parameter of an ideal cubic perovskite and $c_{rs} \approx 1/2a_p$ is the thickness of the rock salt layer. Ca_2MnO_4 ($n=1$) was shown to [4] have a super-cell of $I4/mmm$ unit cell ($a=\sqrt{2}a', c=2c'$). The super-cell results from the c^+ rotations of the MnO_6 octahedra about the axis normal to the layers, which leads to the $I4_1/acd$ space group. $Ca_4Mn_3O_{10-\delta}$ ($n=3$) was determined to adopt the orthorhombic *Pbca* structure with pronounced tilting of MnO_6 octahedra [5], with the tilt system $a^-a^-c^+$, similar to one observed in $CaMnO_3$ [2]. X-ray powder diffraction and Rietveld analysis of RP calcium manganates prepared from citrate gels [6] confirmed the reported structures for Ca_2MnO_4 and $Ca_4Mn_3O_{10}$ and identified the $I4/mmm$ space group (undistorted structure) for $Ca_3Mn_2O_7$.

Our recent study of a series of $La_{2-2x}Ca_{1+2x}Mn_2O_7$ ($0.8 \leqslant x < 1.0$) $n=2$ RP phases by TEM showed

*Corresponding author. Fax: +301-975-4553.
E-mail address: leoben@nist.gov (L.A. Bendersky).

0022-4596/03/$ - see front matter © 2003 Elsevier Inc. All rights reserved.
doi:10.1016/S0022-4596(03)00283-4

Table 1
Crystallographic data for $CaMnO_3$ and $Ca_{n+1}Mn_nO_{3n+1}$

Compound	n	Space group	Lattice parameters	Features	Reference
$CaMnO_3$	∞	*Pnma*	$a = 0.528$ nm, $b = 0.745$ nm, $c = 0.526$ nm	$a^- a^- c^+$ tilt	[2]
Ca_2MnO_4	1	$I4_1/acd$	$a = 0.5183$ nm, $c = 2.411$ nm	$0\,0\,c^+$ tilt, $I4/mmm$-equivalent octahedra are in anti-phase tilt	[4,6]
$Ca_3Mn_2O_7$	2	$I4/mmm$	$a = 0.3683$ nm, $c = 1.9575$ nm	Ideal, no tilt	[6]
$Ca_4Mn_3O_{10}$	3	*Pbca*	$a = 0.5265$ nm, $b = 0.526$ nm, $c = 2.682$ nm	$a^- a^- c^+/a^- a^- c^+$	[5,6]

structural changes apparently occurring in the $I4/mmm$ phase at low temperatures [9]. The low-temperature phase belongs to the non-centrosymmetric space group, $Cmc2_1$. A structural model proposed, based on the $a^- a^- c_z^+/a^- a^- c_z^+$ combination of tilts of octahedra in the perovskite blocks, provided a satisfactory explanation for the observed defects and diffraction extinctions. Based on these results, it is plausible to expect that $Ca_3Mn_2O_7$ also might have a structure different from the ideal $I4/mmm$. Therefore, we performed TEM studies of the $Ca_3Mn_2O_7$ and $Ca_4Mn_3O_{10}$ compounds prepared from citrate gels, and the results are reported in this paper.

2. Experimental procedures

Samples of $Ca_3Mn_2O_7$ and $Ca_4Mn_3O_{10}$ were prepared from $CaCO_3$ (Aldrich[1], 99 + %) and $Mn(NO_3)_2$ (Aldrich, 49.7 wt% solution of dilute nitric acid) by a citrate gel technique. Details of the synthesis are described in Ref. [6]. The powders were pressed into pellets and sintered at 1250°C for 24 h and quenched to room temperature (RT) in air. TEM specimens were prepared from the sintered pellets by conventional methods involving grinding, dimpling and ion thinning. The specimens were examined using JEM3010 and Phillips 430 TEM microscopes operated at 300 and 200 kV, respectively. In all specimens studied a small fraction of an amorphous phase, rich in carbon but including Ca, Mn and O, was observed between the grains of the crystalline phase. The presence of the amorphous phase may introduce some uncertainties in the precise composition of the studied crystalline phases.

3. Experimental results

3.1. $Ca_4Mn_3O_{10}$

Fig. 1 shows two typical selected area electron diffraction (SAED) patterns of $Ca_4Mn_3O_{10}$. The patterns were taken from a twinned region and are indexed as composites of: (a) [110]/[110] and (b) [010]/[100] zone axes, in correspondence with the orthorhombic *Pbca* structure of $Ca_4Mn_3O_{10}$ determined by Battle et al. [5]. Reflection conditions for *Pbca* require $l = 2n$ for $0\,0\,l$ reflections. The visibility of $0\,0\,l$ reflections with odd l on both SAED patterns is the result of double diffraction of electrons; this was confirmed by tilting the TEM specimen around the $[001]^*$ axis (* stands for a reciprocal vector) and observing the disappearance of reflections with odd l. Other reflection conditions of the *Pbca* space group are fulfilled, in particular, the condition for $1\,0\,l: l = 2n$ and $0\,1\,l$: $k = 2n$, as observed for the composite row of $1\,0\,l$ and $0\,1\,l$ reflections, Fig. 1b, and for $1\,\bar{1}\,l$: $l =$ all, Fig. 1c. According to the SAED patterns, the structure of the sol-gel prepared $Ca_4Mn_3O_{10}$ specimens is relatively well ordered but the presence of twin lamellae different in the alternation of **b** and **a** axes is frequently observed. The presence of twins suggests a possible displacive phase transformation by tilting octahedra occurring during cooling of the specimens. Symmetry reduction of the transformation follows the maximal group–subgroup relationship: $I4/mmm \rightarrow Fmmm \rightarrow Abma(Cmca) \rightarrow Pbca$.

Recently, we also studied structures of the $(Ca_{1-x}Sr_x)_4Mn_3O_{10}$ compounds where Ca was partially substituted by Sr ($x = 0.2$ and 0.2875) [7]. In the published SAED patterns of these structures the reflections with odd l for $0\,0\,l$, $2\,0\,l$ and $1\,1\,l$ rows were always absent. This result suggests that the larger Sr^{2+} ions stabilize the structure with respect to the distortion and tilt of the octahedra, and therefore the structures are either not tilted ($I4/mmm$ space group), or form with a single tilt (e.g., $P4_2/ncm$ space group for the tilt system $(a^-\,0\,0)/(0\,a^-\,0)$ [8]).

3.2. $Ca_3Mn_2O_7$

Typical SAED patterns of $Ca_3Mn_2O_7$ are presented in Fig. 2. The patterns are indexed according to the ideal tetragonal (t) $I4/mmm$ structure (Table 1 and Ref. [6]) as: (a) [001], (b) $[010]_t$, (c) $[1\bar{1}0]_t$ and (d) $[1\bar{3}0]_t$ zone axes. Close examination of the patterns reveals diffraction features that suggest a lower symmetry for the phase. In the $[001]_t$ pattern, there are weak spots with

[1] The use of brand or trade names does not imply endorsement of the product by NIST.

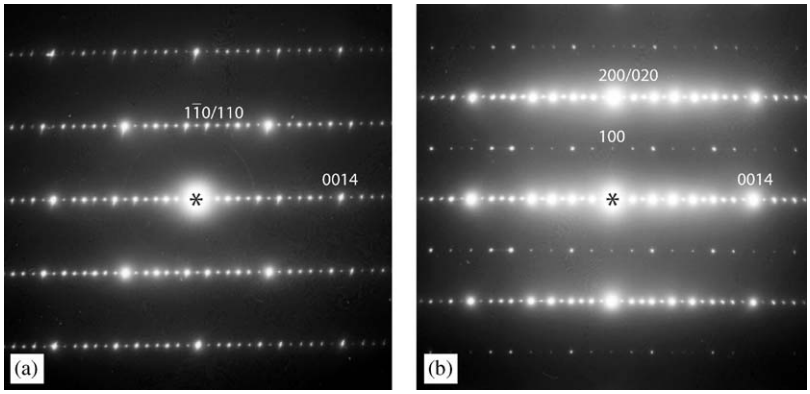

Fig. 1. Two typical SAED patterns of $Ca_4Mn_3O_{10}$. The patterns are indexed according to the orthorhombic lattice of the tilted *Pbca* structure as (a) [110] and (b) composite [010] and [100]. The composite pattern comes from a twinned structure where the twins differ in the alternation of **b** and **a** axes.

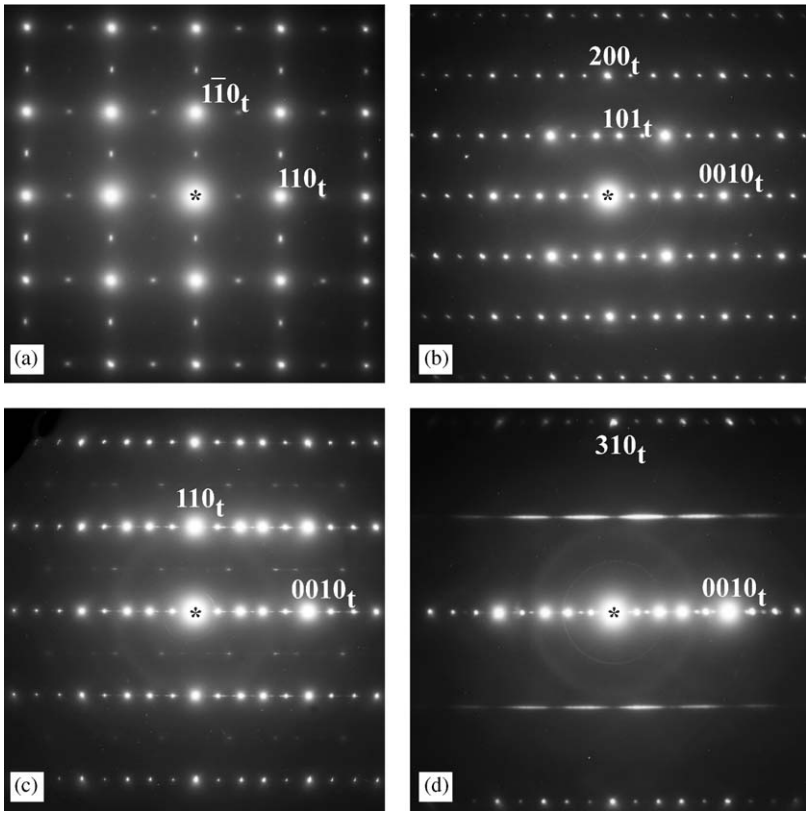

Fig. 2. Typical SAED patterns of $Ca_3Mn_2O_7$. The patterns are indexed as: (a) [001], (b) $[010]_t$, (c) $[1\bar{1}0]_t$ and (d) $[1\bar{3}0]_t$ according to the tetragonal (t) $I4/mmm$ structure (with non-tilted octahedra) (6).

uneven intensity in the $1/2(110)_t$ and $1/2(1\bar{1}0)_t$ positions (Fig 2a). The unevenness of the spots indicates that the spots belong to different crystallographic variants with different volume fraction. In the $[1\bar{1}0]_t$ pattern shown in Fig. 2c, a row of weak $(\frac{1}{2}\frac{1}{2}l)$ reflections with $l = 2n+1$ is observed. However, this additional row of reflections was not observed in all $[1\bar{1}0]_t$-type patterns. The $[1\bar{3}0]_t$ pattern, Fig 2d, is characterized by the presence of a row of near-continuous, modulated intensity along $[\frac{3}{2}\frac{1}{2}l]_t^*$, which suggests a superstructure with either fine domains with $(001)_t$ interfaces or stacking faults on the $(001)_t$ planes. The continuous intensity and its variations suggest the presence of a defect substructure in the form of micro-twins with $(001)_t$ interfaces. The presence of the substructure cannot be seen in a near-zone axis bright field image, Fig. 3a, however a fine lamellar structure is visible in a dark field image, Fig. 3b. The dark field image was obtained by placing an objective aperture on the $[\frac{3}{2}\frac{1}{2}0]_t^*$ diffuse row.

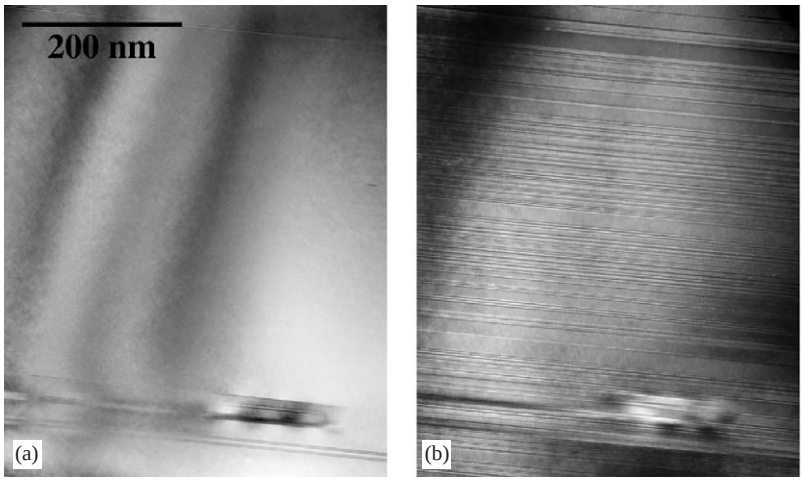

Fig. 3. (a) Bright field and (b) dark field images obtained from the $Ca_3Mn_2O_7$ specimen at near-$[1\bar{3}0]_t$ orientation. The dark field image was obtained by placing an objective aperture in the $[\frac{3}{2}\frac{1}{2}0]_t^*$ position.

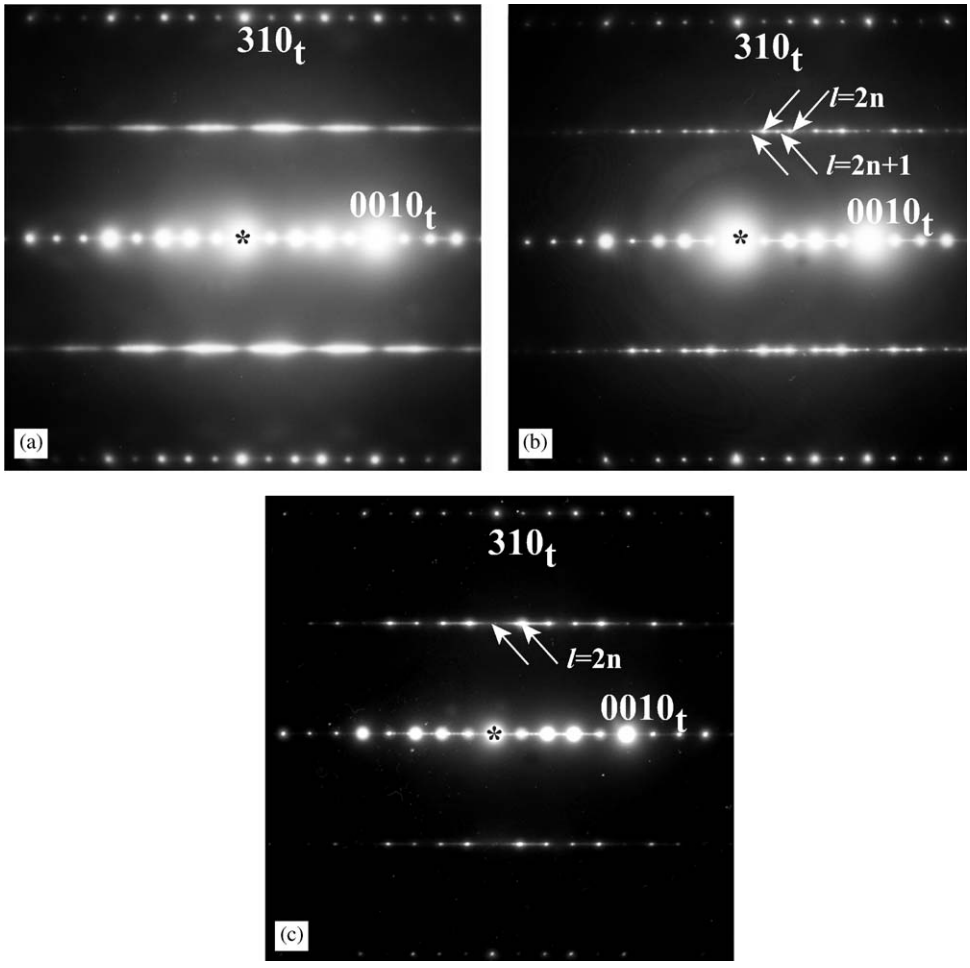

Fig. 4. Three $[310]_t$-type SAED patterns taken from the same TEM specimen but in different locations. (a) the $[\frac{3}{2}\frac{1}{2}l]_t^*$ intensity is continuous; (b) a row of discrete reflections with $l = 2n$ and $l = 2n + 1$; (c) a row of discrete reflections with $l = 2n$.

For some TEM specimens, the intensity along the $[\frac{3}{2}\frac{1}{2}l]_t^*$ row varies significantly. Such variations are shown in Fig. 4 for three SAED patterns taken from the same crystallite but in different locations around a hole. In the (a) pattern the $[\frac{3}{2}\frac{1}{2}l]_t^*$ intensity is continuous, while in the patterns (b) and (c) the discrete reflections can be

recognized. In the pattern (c) the observed reflections appear to have $l = 2n$, whereas in the pattern (b) reflections with both $l = 2n$ and $l = 2n + 1$ are present. The difference in the position of reflections reflects non-equivalency of the $\langle 310 \rangle_t$ patterns, and therefore different extinctions rules for the $(\frac{3}{2}\frac{1}{2}l)_t$ reflections.

The electron diffraction results correspond to an orthorhombic structure with the following lattice relation to the tetragonal $I4/mmm$ cell: $b_o = \sqrt{2}a_t \approx 0.52\,\text{nm}$; $c_o = \sqrt{2}a_t \approx 0.52\,\text{nm}$; $a_o = c_t \approx 1.93\,\text{nm}$ (for a standard setting of the derived orthorhombic space groups a_o is a long axis in the stacking direction). The corresponding reciprocal lattices are schematically drawn in Fig. 5. The reflection conditions for the orthorhombic reciprocal lattice (eliminating the effect of double diffraction) are: $0\,0\,l$: $l = 2n$; $0\,k\,0$: $k = 2n$; $h\,0\,0$: $h = 2n$; $h\,k\,0$: $h + l = 2n$; $h\,0\,l$: $h, l = 2n$; $0\,k\,l$: $k = 2n$; $h\,k\,l$: $h + k = 2n$. The suggested lattice and diffraction features are very similar for the recently studied $La_{2-2x}Ca_{1+2x}Mn_2O_7$ compounds (with $0.8 < x < 1.0$) [9]. Therefore, it is suggested that $Ca_3Mn_2O_7$ and $La_{2-2x}Ca_{1+2x}Mn_2O_7$ have the same crystal structure. For $La_{2-2x}Ca_{1+2x}Mn_2O_7$ two possible space groups, $Cmcm$ and non-centrosymmetric $Cmc2_1$ were proposed. The suggested structural model was based on the tilt of rigid octahedra in the perovskite layers. The $Cmcm$ space group corresponds to the combination of tilts $0b^-b^-/0b^-b^-$, which is equivalent to alternating tilt around the c_o-axis, Fig. 6a. For the $Cmc2_1$ space group, an additional tilt around the a_o-axis is added, Fig. 6b, and the tilt system is $a^+b^-b^-/a^+b^-b^-$. Note that the same tilt system was determined for $Ca_4Mn_3O_{10}$ [5] (see Table 1).

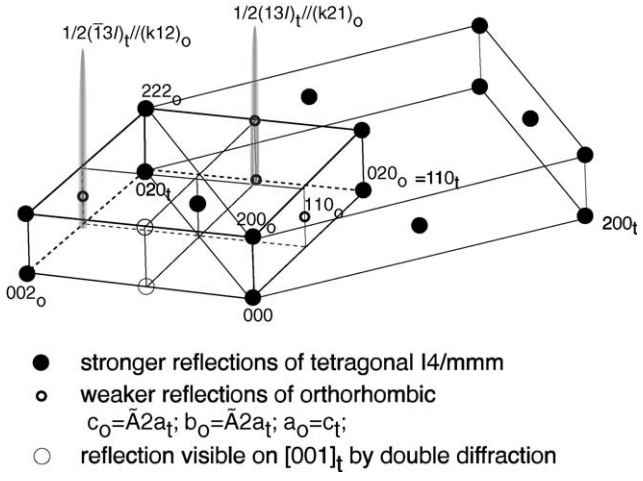

Fig. 5. Schematic drawing showing an orthorhombic reciprocal lattice of $Ca_3Mn_2O_7$ phase according to the electron diffraction experiments. The lattice is derived from the tetragonal $I4/mmm$ (dark circles) and has approximate parameters $a_o = \sqrt{2}a_t = 0.52\,\text{nm}$; $b_o = \sqrt{2}a_t = 0.52\,\text{nm}$; $c_o = c_t = 1.93\,\text{nm}$. Dark-shaded circles represent fundamental reflections of the tetragonal $I4/mmm$, small empty circles—super-lattice of the orthorhombic lattice, large empty circles—kinematically forbidden reflections but observed as a result of double diffraction.

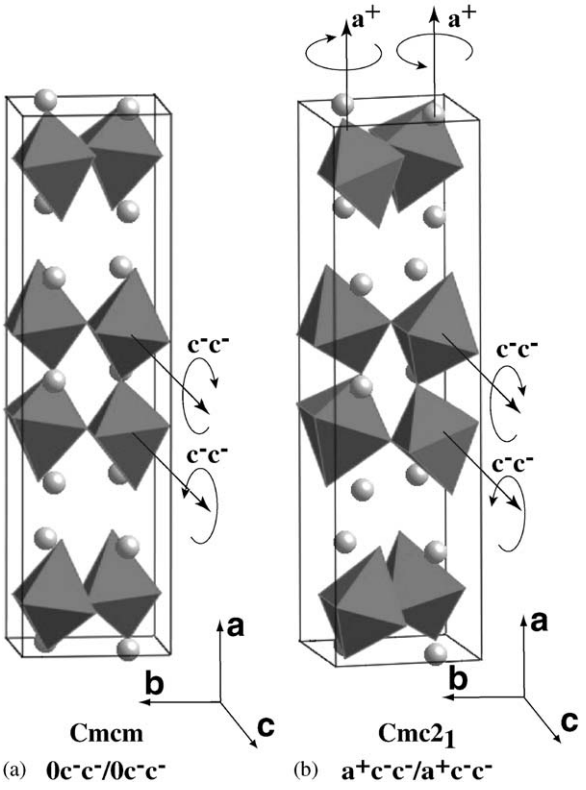

Fig. 6. Drawing of two structural models of $Ca_3Mn_2O_7$. (a) $Cmcm$ with a^-a^-0/a^-a^-0 combination of tilts; (b) $Cmc2_1$ with $a^-a^-c^+/a^-a^-c^+$ combination of tilts.

In order to understand the nature of defects causing the observed continuous intensity, high-resolution TEM images (HRTEM) in the $[310]_t$ orientation (the lowest index zone axis with SAED including the $[\frac{3}{2}\frac{1}{2}l]_t^*$ row of diffuse intensity) were recorded. A typical contrast of the HRTEM images consists of rows of paired bright dots, Fig. 7a. We were able to reproduce such contrast in simulated images for certain combinations of thickness-defocus using the $Cmc2_1$ structural model with 15° angle for both tilts axes. Coordinates of atoms for the model were taken from our model of $Cmc2_1$ structure of $(La,Ca)_3Mn_2O_7$ [9]. According to the simulations, the rows on the HRTEM images correspond to the positions of perovskite blocks, although for such high-index orientation there is no simple structural interpretation of the contrast. Analysis of the HRTEM image Fig. 7a showed the difference in the arrangement of the bright dots in two regions A and B. The arrangement is emphasized by triangles connecting three dots in a paired row, Fig. 7b. In the region A all the triangles along the a_o-direction are pointing in one direction, whereas in the B region direction of the triangles alternates. Fast Fourier transform (FFT) from the regions A and B shows the presence of $[\frac{3}{2}\frac{1}{2}l]_t^*$

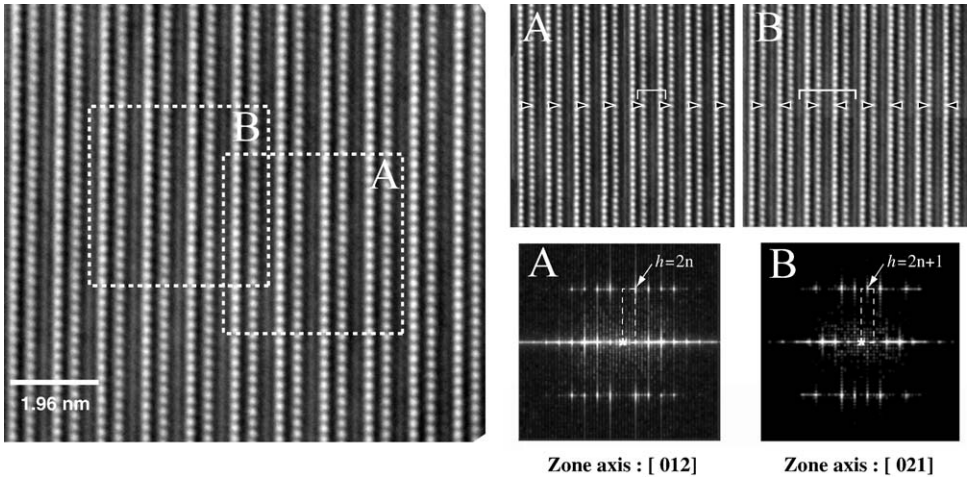

Fig. 7. (a) High-resolution TEM image taken at the $[310]_t$. (b) Analysis of different regions A and B of the $[310]_t$ HRTEM image with respect to the orientation of bright dots (emphasized with triangles). FFT from A and B shows the $[\frac{3}{2}\frac{1}{2}l]^*_t$ reflections with $l = 2n$ and $l = 2n + 1$, and therefore non-equivalent zone axes $[102]_o$ and $[201]_o$ ($c_t = b_o$), respectively.

reflections with either $l = 2n$ or $l = 2n + 1$, respectively. The FFT patterns correspond to the non-equivalent zone axes $[130]_t$ and $[310]_t$ (orthorhombic $[012]_o$ and $[021]_o$) of the $Cmc2_1$ structural model. Therefore, we conclude that the observed defects can be considered as intergrowth of blocks of the orthorhombic $Cmc2_1$ structure with the $(100)_o$ interface. The intergrowth blocks are related to each other by $(110)_t$ mirror reflection, or by permutation of the $\mathbf{a}_t$ and $\mathbf{b}_t$ axes. The presence of the twin-like blocks indicates that a possible phase transition has occurred upon cooling of the material from the sintering temperature 1250°C. The symmetry relationship between two variants of the orthorhombic phase suggests a displacive transition from the tetragonal $I4/mmm$ to either $Cmcm$ or $Cmc2_1$ by tilting of the MnO_6 octahedra. Formally, the symmetry reduction follows the maximal group–subgroup symmetry tree:

$$I4/mmm \rightarrow Fmmm \rightarrow Bbmm(Cmcm) \rightarrow Bb2_1m(Cmc2_1).$$

4. Conclusions

Two RP compounds $Ca_{n+1}Mn_nO_{3n+1}$ with $n = 2$ and 3 synthesized by a citrate gel technique have been studied by TEM. The structure of $Ca_4Mn_3O_{10}$ is consistent with the previously determined structure having the space group $Pbca$ and $a^-\,a^-\,c^+/a^-\,a^-\,c^+$ tilt system. The presence of defects suggests the possible high-temperature phase transition from untilted $I4/mmm$ to $Pbca$.

The structure of $Ca_3Mn_2O_7$ was found to be different from the previously suggested $I4/mmm$ symmetry. $Ca_3Mn_2O_7$ forms with an orthorhombic structure with either $Cmcm$ or $Cmc2_1$ space group. A structural model for $Cmc2_1$ based on the tilting of almost-rigid octahedra with $a^+c^-c^-/a^+c^-c^-$ tilt system is proposed. The lamellar defect were shown to be twin variants of the $Cmc2_1$ structure with the $(001)_t$ interfaces, which suggests the possible tilting phase transition from the ideal $I4/mmm$ to $Cmc2_1$ following the maximal group–subgroup symmetry tree: $I4/mmm \rightarrow Fmmm \rightarrow Bbmm(Cmcm) \rightarrow Bb2_1m(Cmc2_1)$.

Acknowledgment

This work was partially supported (M.G. and R.C.) by NSF-DMR 99-07963 grant.

References

[1] Y. Tokura (Ed.), Colossal Magnetoresistance Oxides, Monograph in Condensed Matter Science, Gordon and Breach, London, 2000.
[2] K.R. Poeppelmeier, M.E. Leonowicz, J.C. Scanlon, J.M. Longo, W.B. Yelon, J. Solid State Chem. 45 (1982) 71.
[3] M. Glazer, Acta Crystallogr. B 28 (1975) 3385.
[4] M.E. Leonowicz, K.R. Poeppelmeier, J.M. Longo, J. Solid State Chem. 71 (1985) 59.
[5] P.D. Battle, M.A. Green, J. Lago, J.E. Millburn, M.J. Rosseinsky, J.F. Vente, Chem. Mater. 10 (1998) 658.
[6] I.D. Fawcett, J.E. Sunstrom IV, M. Greenblatt, M. Croft, K.V. Ramanujachary, Chem. Mater. 10 (1998) 3643.
[7] R. Chen, M. Greenblatt, L.A. Bendersky, Chem. Mater. 13 (2001) 4094.
[8] K.S. Aleksandrov, B.V. Besnosikov, Perovskitopodobnie kristalli, Novosibirsk, Nauka, 1997 (in Russian).
[9] L.A. Bendersky, R. Chen, I.D. Fawcett, M. Greenblatt, J. Solid State Chem. 157 (2001) 309.